

# Mycophenolate Mofetil Inhibits Regenerative Repair in Uranyl Acetate-Induced Acute Renal Failure by Reduced Interstitial Cellular Response

Di Fei Sun,\* Yoshihide Fujigaki,\* Taiki Fujimoto,\* Tetsuo Goto,\* Katsuhiko Yonemura,† and Akira Hishida\*

From the First Department of Medicine\* and the Hemodialysis Unit,† Hamamatsu University School of Medicine, Hamamatsu, Shizuoka, Japan

**We recently reported that transient appearance of interstitial myofibroblasts and infiltrating macrophages might play a role in cellular recovery in uranyl acetate (UA)-induced acute renal failure (ARF). Here we tested the effects of mycophenolate mofetil (MMF), which attenuates infiltration of lymphocytes, macrophages, and myofibroblasts, but does not suppress epithelial regeneration, on renal tissue repair. Rats treated with MMF (20 mg/kg/day) or vehicle were sacrificed at 2, 5, and 7 days after induction of ARF by injection of 5 mg/kg UA. Renal tissues were immunostained for bromodeoxyuridine (BrdU) and Ki67,  $\alpha$ -smooth muscle actin ( $\alpha$ -SMA), ED1, and CD43. The expression levels of  $\alpha$ -SMA mRNA were examined by reverse transcription-polymerase chain reaction. Body weight loss or serum albumin levels were similar in MMF and vehicle rats during the experiment. In vehicle group, serum creatinine (Scr) significantly increased after day 5, but proximal tubular (PT) damage score increased as early as day 2 after UA injection. BrdU- or Ki67-positive regenerating tubular cells, ED1-positive macrophages and  $\alpha$ -SMA-positive myofibroblasts significantly increased in the interstitium after day 5. In MMF-treated rats, Scr and PT damage score significantly increased at day 7 and the number of regenerating PT were significantly reduced compared with vehicle-treated rats at days 5 and 7. The numbers of macrophages and myofibroblasts and the expression of  $\alpha$ -SMA mRNA were significantly lower in MMF than in vehicle rats at day 5, indicating that reduced interstitial cellular response is linked to the inhibition of regenerative repair. CD43-positive lymphocytes were significantly reduced in MMF group than in vehicle group at day 7, suggesting that lymphocyte infiltration does not seem to contribute to early regenerative response of proximal tubules. The transient appearance of myofibroblasts and macrophages in the interstitium may promote regenera-**

**tive repair in UA-induced ARF in rats. (Am J Pathol 2002, 161:217–227)**

Myofibroblasts and infiltrating macrophages are known to contribute to the process of wound healing.<sup>1–4</sup> Cellular recovery after acute renal failure (ARF) is a unique form of wound healing, and complete regenerative repair is sometimes possible. This indicates that interstitial myofibroblasts and macrophages may participate in the regenerative repair in ARF based on their potential roles in wound healing.<sup>5,6</sup> Using an animal model of ARF induced by uranyl acetate (UA), we recently reported the transient appearance of  $\alpha$ -smooth muscle actin ( $\alpha$ -SMA)-positive myofibroblasts and monocytes/macrophages in the renal interstitium, and the formation of myofibroblast network that surrounds denuded tubular basement membrane (TBM), which remained in place until cellular recovery was completed.<sup>7</sup> The role of the transient appearance of myofibroblasts in this setting is unknown, but we speculated that myofibroblasts might serve to provide contractility to prevent the collapse of the nephron, furnish extracellular matrix (ECM), and enhance the production of cytokines to promote cellular recovery. Transient infiltration of monocytes/macrophages in ARF can be considered to be one of sources for cytokines that do not only damage tubules but also promote cellular recovery. However, in our previous study,<sup>7</sup> we did not provide a direct evidence for the role of interstitial cellular response in ARF.

Mycophenolate mofetil (MMF) is a specific inhibitor of inosine monophosphate dehydrogenase, an enzyme involved in *de novo* purine synthesis, thereby exerting a selective anti-proliferative activity on lymphocytes and monocytes and used as an immunosuppressive agent.<sup>8</sup> In addition, MMF has an effect on cells outside of the immune system and particularly an anti-proliferative effect on vascular SMA *in vivo* and *in vitro*.<sup>9</sup> It is also re-

Supported by research grant 13671107 from the Ministry of Education, Science, Sports, and Culture in Japan.

This study was presented in abstract form at The World Congress of Nephrology, San Francisco, CA, 2001.

Accepted for publication April 15, 2002.

Address reprint requests to Yoshihide Fujigaki, M.D., The First Department of Medicine, Hamamatsu University School of Medicine, 1-20-1 Handayama, 431-3192 Hamamatsu, Japan. E-mail: yf0516@hama-med.ac.jp.

ported that MMF inhibits myofibroblasts infiltration and/or differentiation in rat remnant kidney.<sup>10</sup> On the other hand, other studies showed that MMF did not inhibit tubular regeneration in renal ischemia/reperfusion injury in rats<sup>11</sup> or liver regeneration in rats.<sup>12</sup>

In the present study, we used MMF to suppress the infiltration of macrophages and myofibroblasts in the renal interstitium. Our results showed that MMF inhibited the infiltration of both macrophages and myofibroblasts in the renal interstitium, and that MMF simultaneously inhibited regeneration of tubular epithelial cells. Our findings suggest that the transient interstitial cellular response could promote the regenerative repair in UA-induced ARF.

## Materials and Methods

### Experimental Design

A total of 42 male Sprague-Dawley rats weighing 200 to 250 g (SLC Co., Shizuoka, Japan) were used in the present study. Rats had free access to standard rat chow and drinking water. All rats received a single intravenous injection of 5 mg/kg of UA via the dorsal penile vein. After induction of ARF, the rats were divided into two groups: the first group received 20 mg/kg of MMF (Roche Laboratories, Palo Alto, CA) by daily gastric gavage, while the second group received the same volume of vehicle by the same route of administration. According to the instructions provided by the manufacturer, vehicle solution, pH 3.5, was prepared using benzyl alcohol, polysorbate 80, sodium carboxymethylcellulose, NaCl, and water. Before gavage, MMF was added to the vehicle solution to a final concentration of 4 mg/ml, followed by sonication. Six rats in each group were sacrificed at days 2, 5, and 7 after UA injection and six rats without any treatment were used as normal control. Body weight was measured before UA administration and at sacrifice. To label cells that actively synthesize DNA, all rats were injected intraperitoneally with 40 mg/kg of bromodeoxyuridine (BrdU) (Sigma Chemicals Co., St. Louis, MO), 1 hour before sacrifice. Rats were anesthetized with intraperitoneal administration of pentobarbital sodium (30 mg/kg body weight), and a blood sample was collected through the abdominal aorta. Then both kidneys were dissected out after a brief flush with phosphate-buffered saline (PBS) for histological examinations. Serum creatinine (Scr) level was measured by the enzymatic method (Mizuho Med, Saga, Japan), and serum albumin level was determined by enzyme-linked immunosorbent assay using rat serum albumin as a standard.<sup>13</sup>

### Tissue Preparation

Both kidneys were bisected through longitudinal axis. One half of the left kidney was fixed with methacarn solution, followed by paraffin embedding, and the rest was snap-frozen into liquid nitrogen and stored at  $-70^{\circ}\text{C}$  for RNA extraction. The right kidney was fixed with 4% paraformaldehyde then embedded in paraffin.

### Histochemistry and Immunohistochemistry

For histological examination of renal tissues, 4- $\mu\text{m}$ -thick sections were stained with periodic acid-Schiff. Standardized avidin-biotin-complex technique was applied to detect the following antibodies: mouse monoclonal antibody against BrdU (Amersham International, Poole, UK) and mouse monoclonal antibody against Ki67 (Novocastria, Newcastle on Tyne, UK), both as cell proliferation markers; mouse monoclonal antibody against human  $\alpha$ -SMA (DAKO, Glostrup, Denmark) as myofibroblast phenotypic marker; mouse monoclonal antibody against ED1 (Serotec, Oxford, UK) as rat monocytes/macrophages and mouse monoclonal antibody against CD43 (Cosmobio, Tokyo, Japan) as rat lymphocytes. Briefly, 4% paraformaldehyde (for BrdU, Ki67, and  $\alpha$ -SMA)-, methacarn (for ED1 and CD43)-fixed sections were deparaffinized and dehydrated. Endogenous peroxidase was blocked by treatment with 3%  $\text{H}_2\text{O}_2$  for 30 minutes, then the sections were incubated with 10% normal donkey serum for 20 minutes, followed by incubation with first antibodies overnight at  $4^{\circ}\text{C}$  (except BrdU and Ki67 at  $37^{\circ}\text{C}$ ). After rinsing with PBS, sections were incubated with biotinylated donkey anti-mouse IgG (Chemicon International Inc., Temecula, CA) for 30 minutes at room temperature. Then streptavidin-conjugated peroxidase (Nichirei, Tokyo, Japan) was added for 30 minutes, and then the reaction product was visualized by incubation with diaminobenzidine. Counterstaining was performed by using hematoxylin. For histochemical control sections, the first antibodies were omitted or replaced by normal serum of corresponding animal. Signals in both normal control and experimental sections were negative or negligible.

### Morphometric Analysis

#### Proximal Tubular (PT) Damage

The degree of PT damage in the outer stripe of outer medulla (OSOM) was assessed on periodic acid-Schiff-stained sections at  $\times 400$  magnification using 20 randomly selected fields. Tubular injury was categorized into one of five grades using following criteria reported by Houghton and colleagues<sup>14</sup> with some modifications: grade 0, normal; grade 1, tubular cells exhibiting desquamation from TBM and/or granulovascular degeneration are  $<25\%$  of individual tubules in a cluster; grade 2, 25 to 50% tubular cells are involved; grade 3, 50 to 75%; and grade 4, 75 to 100%. The mean score in each rat represented the average score of examined 20 high-power fields.

#### Number of BrdU- or Ki67-Positive Cells, ED 1-Positive Monocytes/Macrophages, and CD43-Positive Lymphocytes

For semiquantitative analysis, the number of BrdU-positive PT cells, of Ki67-positive PT and interstitial cells, of ED 1-positive cells and of CD43-positive cells in OSOM

was counted at  $\times 400$  magnification. The number of each type of immunoreactive cells in each rat represented the average number of 50 fields examined and the mean number at days 0, 2, 5, and 7 in each group was displayed in histograms.

#### $\alpha$ -SMA-Positive Area

For semiquantification of  $\alpha$ -SMA-positive area in OSOM in each group, point counting was performed using the method reported by Badid and colleagues.<sup>2</sup> A total of 20 high-power fields at  $\times 400$  magnification per section were counted in each animal. The percentage of fractional area (percentage of positive area relative to the total area counted in the section) was calculated using the following formula: percentage of fractional area = number of grid intersections with positive staining/total number of grid intersections  $\times 100$ .

#### $\alpha$ -SMA mRNA

Total RNA was extracted from the frozen kidney (the whole kidney except papilla and inner medulla) using the Isogen RNA Isolation Kit (Nippongene Inc., Tokyo, Japan) using the instructions provided by the manufacturer. Extracted RNA with an OD<sub>260</sub>/OD<sub>280</sub> ratio by UV spectrophotometry of  $>1.8$  was used for cDNA synthesis.

First-strand cDNA was synthesized with cDNA synthesis kit (Roche Diagnostics Corp., Indianapolis, IN) using 2  $\mu$ g of total RNA in 20  $\mu$ l of reaction solution, 1  $\mu$ l of each cDNA was provided for polymerase chain reaction (PCR) and amplified in a total volume of 25  $\mu$ l containing PCR buffer, 1.5 mmol/L MgCl<sub>2</sub>, 200  $\mu$ mol/L of each dNTP, 0.4  $\mu$ mol/L of each primer, and 1.25 U of *Taq*DNA polymerase (AmpliTaq Gold with Gene Amp; Applied Biosystems, Foster City, CA). To quantitate PCR products and to confirm the integrity of RNAs, a housekeeping gene, glyceraldehyde-3-phosphate dehydrogenase (GAPDH) was co-amplified. We used the reported primers of  $\alpha$ -SMA: 5'-CGATAGAACACGGCATCATC (sense) and 5'-CATCAGGCAGTTCGTAGCTC (anti-sense) to yield a 525-bp product<sup>15</sup> and of GAPDH: 5'-AATGCATCCTG-CACCACCAA (sense) and 5'-GTAGCCATATTCATTGT-CATA (anti-sense) to yield a 515-bp product.<sup>16</sup> PCR was performed with a DNA thermal cycler (MJ Research Inc., Watertown, MA) using the following program: 94°C for 1 minute, 60°C for 1 minute, and 72°C for 2 minutes. Amplification was performed at 35 cycles with both  $\alpha$ -SMA and GAPDH primers. PCR products (6  $\mu$ l) were electrophoresed through a 2% agarose gel with ethidium bromide (Sigma Chemical Co., St. Louis, MO). The DNA bands were visualized under ultraviolet light and photographed. The density of each DNA band was measured with NIH Image software and the mRNA levels for  $\alpha$ -SMA were expressed as a ratio of the optical density units relative to GAPDH.

#### Statistical Analysis

Data are expressed as mean  $\pm$  SEM. Differences between data sets were examined for statistical significance

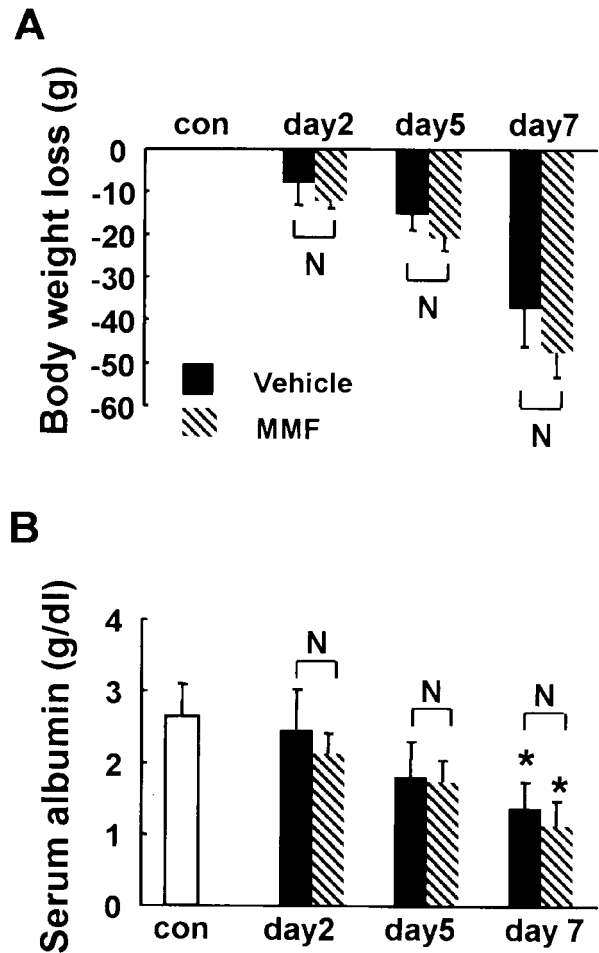


**Figure 1.** Body weight loss (A) and serum albumin (B) in MMF- and vehicle-treated rats. Data represent the mean  $\pm$  SEM values of six animals. \*,  $P < 0.05$  versus normal control (con); \*\*,  $P < 0.001$  versus normal control; N, no significant difference.

using one-way analysis of variance followed by Fisher's *t*-test. Comparison between values for MMF group and vehicle group was performed using paired *t*-test. Correlation coefficients were determined using Spearman's rank order. A *P* level  $<0.05$  was accepted as statistically significant.

## Results

### General Condition

In our preliminary study, normal rats ( $n = 4$ ) treated with 20 mg/kg/day of MMF were able to survive without any clinical symptoms for at least 21 days, but all rats with UA-induced ARF ( $n = 4$ ) treated with the same dose of MMF died at day 9, suffering from severe diarrhea. Therefore, in the present study, the experimental period was limited to day 7 after ARF induction.

After induction of ARF, body weight progressively decreased but there was no significant difference in body weight loss between rats of MMF and vehicle groups at each time point (Figure 1A). Serum albumin level was also significantly lower in rats of both groups, compared



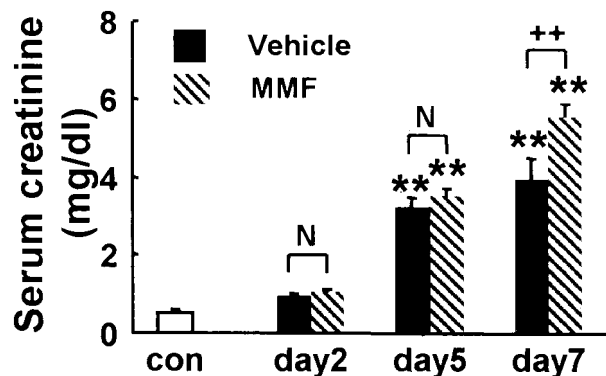


**Figure 2.** Scr in MMF- and vehicle-treated rats. Data represent the mean  $\pm$  SEM values of six rats. \*\*,  $P < 0.001$  versus normal control (con); N, no significant difference; ++,  $P < 0.001$ .

with that of normal control at day 7, but no significant difference was found between both groups at each time point (Figure 1B).

### Serum Creatinine

Scr increased significantly in both MMF and vehicle groups at days 5 and 7 when compared with that in normal control. There was no significant difference in Scr between rats of both groups at days 2 and 5, but Scr was significantly higher in rats of MMF group at day 7 than in the vehicle group (Figure 2).

### Changes in Proximal Tubules

Periodic acid-Schiff-stained sections showed severe necrosis of PT mainly at the corticomedullary junction at day 2 (data not shown) and wide distribution of PT necrosis and cellular debris in the lumen of OSOM at day 5 in both MMF and vehicle groups (Figure 3, A and B). In the vehicle group at day 7, the majority of necrotic tubules with denuded TBM were covered by regenerating PTs with flattened cytoplasm and hyperproliferative PTs were sometimes observed although a few clusters of severely damaged tubules still existed (Figure 3C). In contrast, at day 7 in MMF group, denuded TBM was still noted in most PTs with cellular debris in the lumen but only a few regenerative PTs could be seen (Figure 3D).

Morphometric analysis revealed no difference in PT damage score between rats in both groups at days 2 and 5. However, PT damage score was significantly higher in rats of MMF group at day 7 than in the respective vehicle group (Figure 4).

### Proliferation of PT Cells and Interstitial Cells

As we reported previously,<sup>7</sup> regenerating PT cells indicated by BrdU or Ki67 positivity were found at the border zone between OSOM and inner stripe of the outer medulla at day 2 in both groups (data not shown). In the vehicle group, BrdU- or Ki67-positive PT cells equivalently distributed in OSOM at day 5 (Figure 5, A and C),

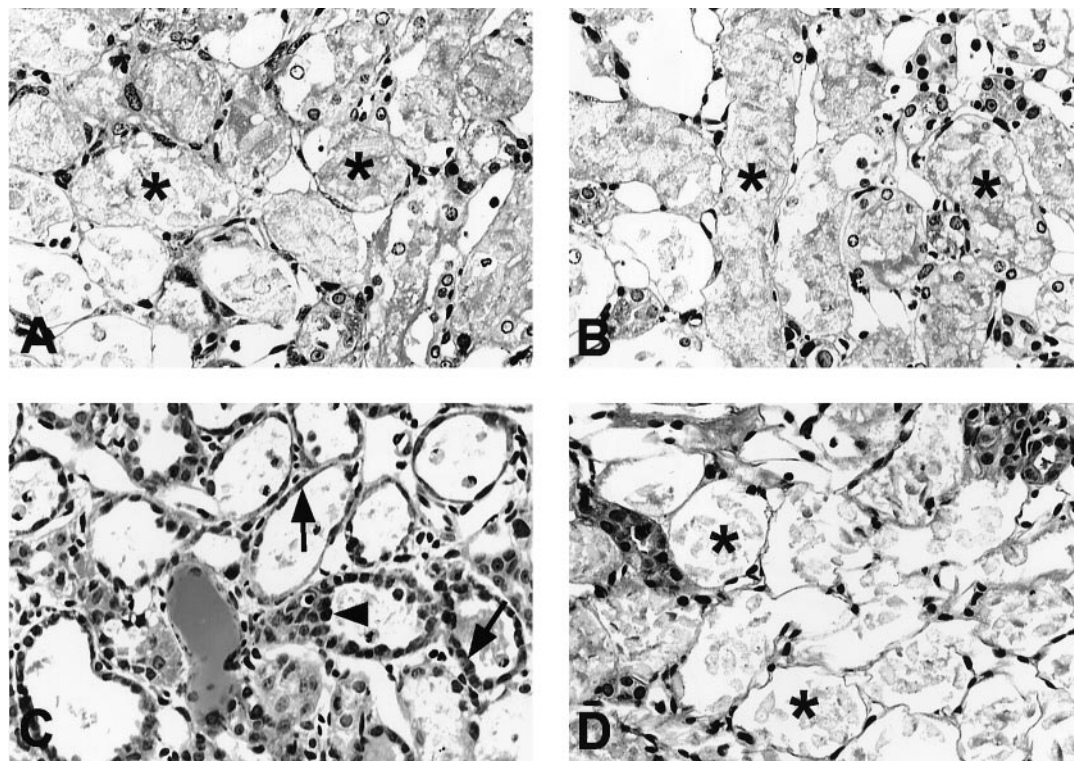


**Figure 3.** Photomicrographs of periodic acid-Schiff-stained sections in the OSOM in vehicle-treated (A, C) and MMF-treated (B, D) rats at days 5 (A, B) and 7 (C, D) after induction of ARF. Damaged proximal tubules with bare TBM (asterisks) were almost maximally distributed in OSOM at day 5 in both groups. At day 7, damaged proximal tubules with bare TBM were still predominant in MMF-treated rats, whereas regenerating cells (arrows) covered most of the TBM and hyperproliferative proximal tubules (arrowhead) could be found in vehicle-treated rats. Original magnifications,  $\times 300$ .

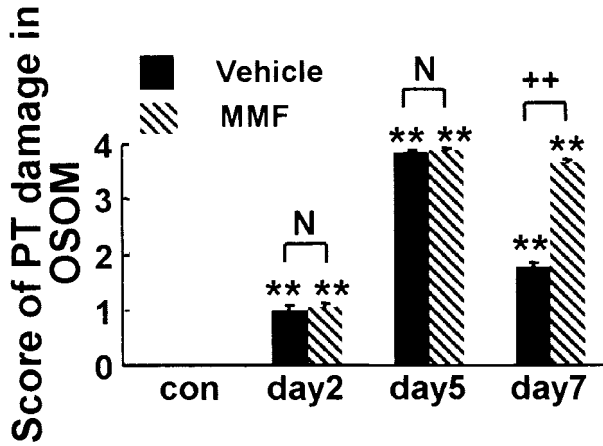


**Figure 4.** The PT damage score in OSOM. Data represent the mean  $\pm$  SEM values of six rats. \*\*,  $P < 0.001$  versus normal control (con); N, no significant difference; ++,  $P < 0.001$ .

and almost covered the denuded TBM at day 7 (Figure 5E). On the other hand, in the MMF group, only a small number of BrdU-positive or Ki67-positive PT cells were distributed sporadically in OSOM at days 5 and 7 (Figure 5; B, D, and F). Morphometric analysis revealed that the numbers of BrdU- or Ki67-positive PT cells were significantly lower at days 5 and 7 in the MMF group than the vehicle group at the respective time intervals (Figure 6, A and B).

In the interstitium, BrdU positivity was not prominent in our ARF model, but we could not exclude the lack of incorporation of BrdU into interstitial cells. Thus, we used another proliferation marker, Ki67, to examine whether there is any difference of proliferative activity of interstitial cells between groups. The number of Ki67-positive interstitial cells significantly increased in vehicle group at day 5 compared to day 2 and control groups (Figures 5C and 6B). The numbers of Ki67-positive interstitial cells at days

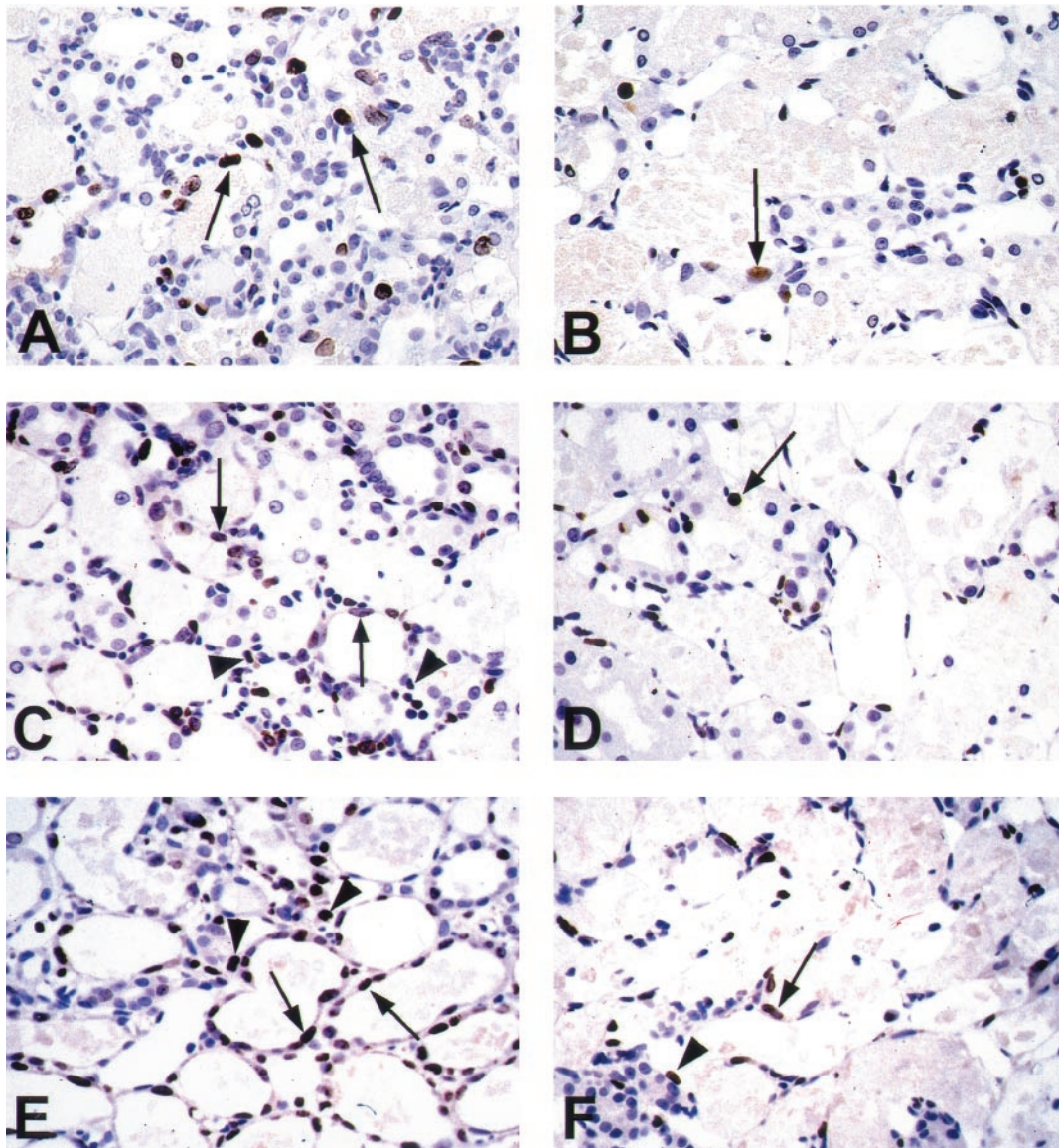


**Figure 5.** Photomicrographs of immunostaining for BrdU (A, B) and Ki67 (C-F) in OSOM in vehicle-treated (A, C, and E) and MMF-treated (B, D, and F) rats at days 5 (A-D) and 7 (E, F) after induction of ARF. **Arrows**, immunoreactive tubular cells; **arrowheads**, immunoreactive interstitial cells. Original magnifications,  $\times 320$ .



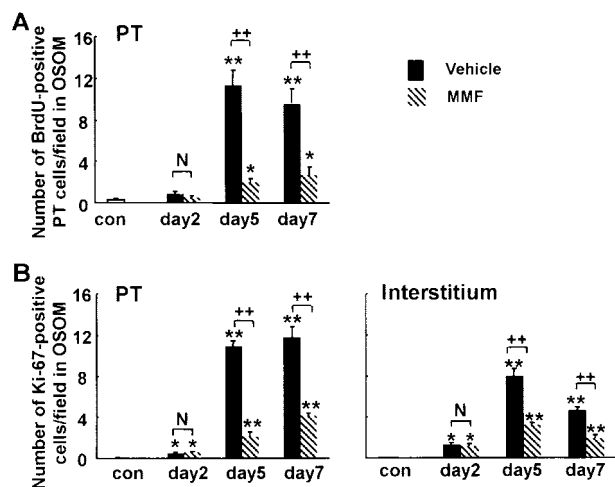


**Figure 6.** **A:** The number of BrdU-positive cells in proximal tubules (PT) per field in the OSOM. **B:** The number of Ki67-positive cells in proximal tubules (PT) or interstitium per field in the OSOM. Data represents the mean  $\pm$  SEM values of six rats. \*,  $P < 0.05$  versus normal control (con); \*\*,  $P < 0.001$  versus normal control; N, no significant difference; ++,  $P < 0.001$ .

5 and 7 were significantly lower in MMF group compared with the vehicle group at the respective days (Figure 5, C to F, and Figure 6B).

### Interstitial Myofibroblasts and Expression of $\alpha$ -SMA mRNA

In normal rats, no or only a few  $\alpha$ -SMA-positive cells were detected in the interstitium except in vascular smooth muscles (data not shown). After induction of ARF,  $\alpha$ -SMA-positive myofibroblasts were found in the corticomedullary region, exclusively around damaged tubules with denuded TBM at day 2 and the staining pattern of  $\alpha$ -SMA was similar between the groups (data not shown).  $\alpha$ -SMA-positive myofibroblasts formed a network around the damaged tubules in the OSOM in the vehicle group at days 5 and 7 (Figure 7A). In contrast, the staining intensity of  $\alpha$ -SMA was relatively weak or faint in MMF group at days 5 and 7 (Figure 7B).

Morphometric analysis revealed that the relative area stained for  $\alpha$ -SMA was significantly lower in the MMF group at days 5 and 7 compared with the vehicle group at the corresponding time intervals (Figure 8A). Further analysis showed that the expression of  $\alpha$ -SMA mRNA was significantly higher in vehicle groups at days 5 and 7 (Figure 8B), however, it was significantly lower in the MMF group at day 5 than in the vehicle group at day 5, but there was no difference between groups at days 2 and 7, respectively (Figure 8B).

Relative area stained for  $\alpha$ -SMA was significantly related both to Scr ( $r = 0.81$  in vehicle group,  $P < 0.01$ ;  $r = 0.80$  in MMF group,  $P < 0.01$ ) and to PT damage score ( $r = 0.73$  in vehicle group,  $P < 0.01$ ;  $r = 0.65$  in MMF group,  $P < 0.05$ ) until day 7 after UA injection in both groups (Figure 9). Even when the functional (Scr) or morphological (PT damage score) damages are almost the same, individual values of  $\alpha$ -SMA-stained area tend to be lower in the MMF group than in vehicle group

(Figure 9), suggesting that  $\alpha$ -SMA-positive myofibroblast infiltration was inhibited despite established kidney damage in the MMF group.

### Interstitial Infiltrating Macrophages and Lymphocytes

In normal rats, ED1-positive monocytes/macrophages were found only occasionally in the interstitium (data not shown). After induction of ARF, the number of ED1-positive cells was significantly increased in both MMF and vehicle groups at days 5 and 7 (Figure 7, C and D, and Figure 10A). However, it was significantly lower in the MMF group only at day 5 than in the vehicle group (Figure 7, C and D, and Figure 10A). Number of ED1-positive cells was significantly related both to Scr ( $r = 0.78$  in the vehicle group,  $P < 0.01$ ;  $r = 0.78$  in the MMF group,  $P < 0.01$ ) and to PT damage score ( $r = 0.76$  in the vehicle group,  $P < 0.01$ ;  $r = 0.59$  in the MMF group,  $P < 0.05$ ).

In normal rats, CD43-positive lymphocytes were scarce in the interstitium (data not shown). After induction of ARF, the number of CD43-positive lymphocytes was significantly increased at day 5 in both groups and at day 7 in the vehicle group (Figure 7, E and F, and Figure 10B), but it was significantly lower in the MMF group at day 7 than in the vehicle group at day 7 (Figure 10B). Number of CD43-positive cells was significantly related both to Scr and to PT damage score in the vehicle group ( $r = 0.63$  for Scr,  $P < 0.05$ ;  $r = 0.57$  for PT damage,  $P < 0.05$ ) but not in the MMF group.

### Discussion

The mechanisms underlying cellular recovery after ARF are complex and primarily unknown. Cellular recovery after ARF is a unique form of wound healing. In general, myofibroblasts associated with infiltrating macrophages are known to contribute to wound healing.<sup>1-4</sup> We recently reported the transient appearance of  $\alpha$ -SMA-positive myofibroblasts and ED1-positive macrophages in the renal interstitium during the recovery phase of UA-induced ARF in rats.<sup>7</sup> The natural course of this ARF model reported previously by us<sup>7</sup> is as follows. Necrotic PT initially appeared around the corticomedullary junction as early as day 2 after UA injection, then almost maximally spread in cortex and OSOM between days 4 and 5. Scr increased as early as day 3, reached a peak value at day 7, then returned to a normal level by day 15. Peritubular  $\alpha$ -SMA-positive myofibroblasts appeared as early as day 2 and formed network throughout cortex and OSOM at days 4 to 5, which remained in place until cellular recovery completed. Tubular regeneration originated in the distal end of PT at day 2, then upstream proliferation of PT cells was noted along TBM firmly attached by myofibroblasts, and denuded TBM were almost covered with regenerating cells by day 7. ED 1-positive infiltrating macrophages increased in the region of injury, reached a peak value around day 5, then gradually disappeared after tubules have regenerated. In the present study, we

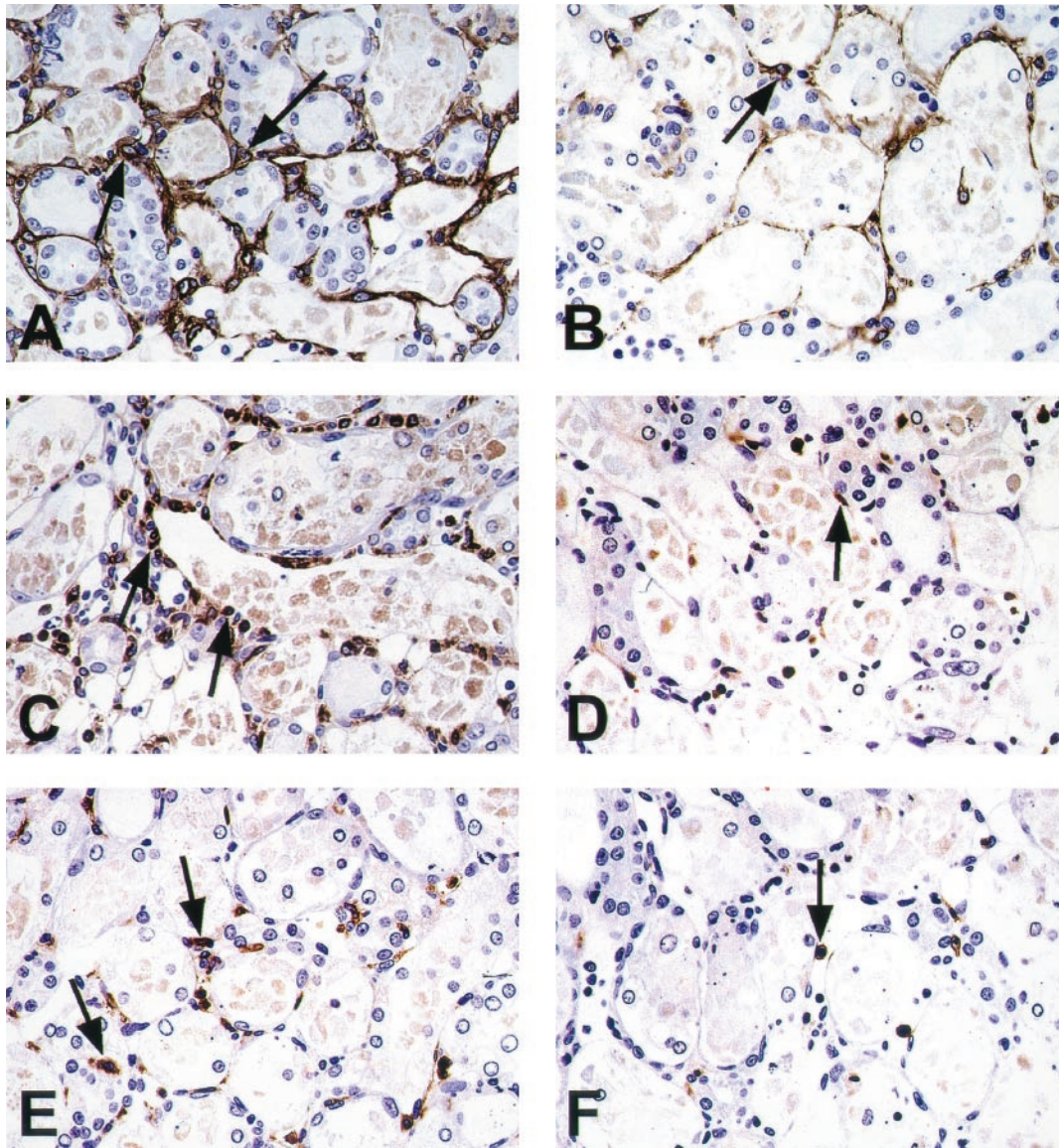


**Figure 7.** Photomicrographs of immunostaining for  $\alpha$ -SMA (A, B), ED1 (C, D), and CD43 (E, F) in the OSOM in vehicle-treated (A, C, and E) and MMF-treated (B, D, and F) rats at days 5 (A–D) and 7 (E, F). **Arrows**,  $\alpha$ -SMA-positive myofibroblasts (A, B), ED1-positive macrophages (C, D), or CD43-positive lymphocytes (E, F). Original magnifications,  $\times 300$ .

determined the role of the interstitial cellular response on cellular recovery using this ARF model. The major findings of our study were the following: MMF treatment decreased interstitial infiltration of macrophages and lymphocytes as well as myofibroblasts, and inhibited the regenerative repair of PT and aggravated renal dysfunction compared with vehicle-treated rats.

MMF is a known suppressor of proliferation of both T and B lymphocytes and monocytes<sup>17</sup> and is also known to have an anti-proliferative effect on vascular smooth muscle cells *in vivo* and *in vitro*.<sup>9</sup> In the kidney, MMF was reported to attenuate infiltration of T lymphocytes and macrophages in the renal interstitium and ameliorate the progression of renal dysfunction in a chronic renal disease model (subtotal nephrectomy) in rats.<sup>18</sup> Recently Badid and colleagues<sup>10</sup> reported that MMF treatment significantly improved renal function and reduced com-

pensatory hypertrophy of the remnant kidney, cell proliferation, myofibroblast infiltration, and collagen III deposition after subtotal nephrectomy in rats.<sup>10</sup> In addition, it is reported that mycophenolic acid exhibits a dose-dependent inhibitory effect on the proliferation of rat fibroblasts *in vitro*.<sup>10</sup> Therefore, we used MMF to suppress interstitial infiltration of macrophages and myofibroblasts in the present study. The dose of MMF used in our study was within the range of the reported dose (10 to 30 mg/kg/day) commonly used in rats. However, in our preliminary study, ARF rats treated with 20 mg/kg/day MMF died with diarrhea at day 9. The cause of death may be explained by two scenarios. *In vivo*, MMF is rapidly converted to mycophenolic acid, its pharmacologically active metabolite, and excreted rapidly into urine as mycophenolic acid glucuronide, the inactive and primary metabolite of mycophenolic acid.<sup>19</sup> Thus, it is possible that death was

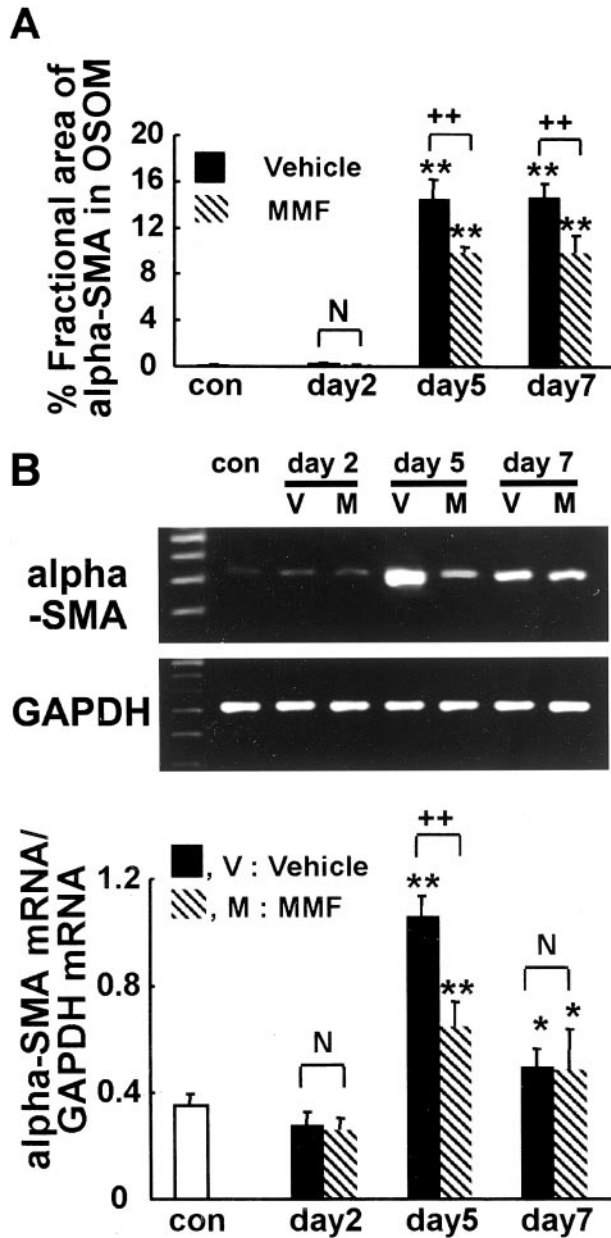


**Figure 8. A:** Morphometric analysis of fractional area of  $\alpha$ -SMA in OSOM in MMF-treated and vehicle-treated rats. **B:** Ratio of  $\alpha$ -SMA to GAPDH mRNA in the kidney in MMF-treated and vehicle-treated rats. Data represent the mean  $\pm$  SEM values of six rats. \*,  $P < 0.05$  versus normal control (con); \*\*,  $P < 0.001$  versus normal control; N, no significant difference; ++,  $P < 0.001$ .

because of a direct toxicity of mycophenolic acid, an active metabolite of MMF, caused by increased serum concentrations of mycophenolic acid in renal failure. However, this seems unlikely because the mycophenolic acid clearance is not affected by reduced renal function.<sup>19,20</sup> Furthermore, the body weight loss and serum albumin level, as parameters of nutritional condition were equivalent in MMF and vehicle groups in our experiments and ischemic ARF rats treated with 40 mg/kg/day of MMF were reported to show no toxic effect until day 7.<sup>11</sup> The other possible cause of death is uremia caused by lack of recovery from ARF.

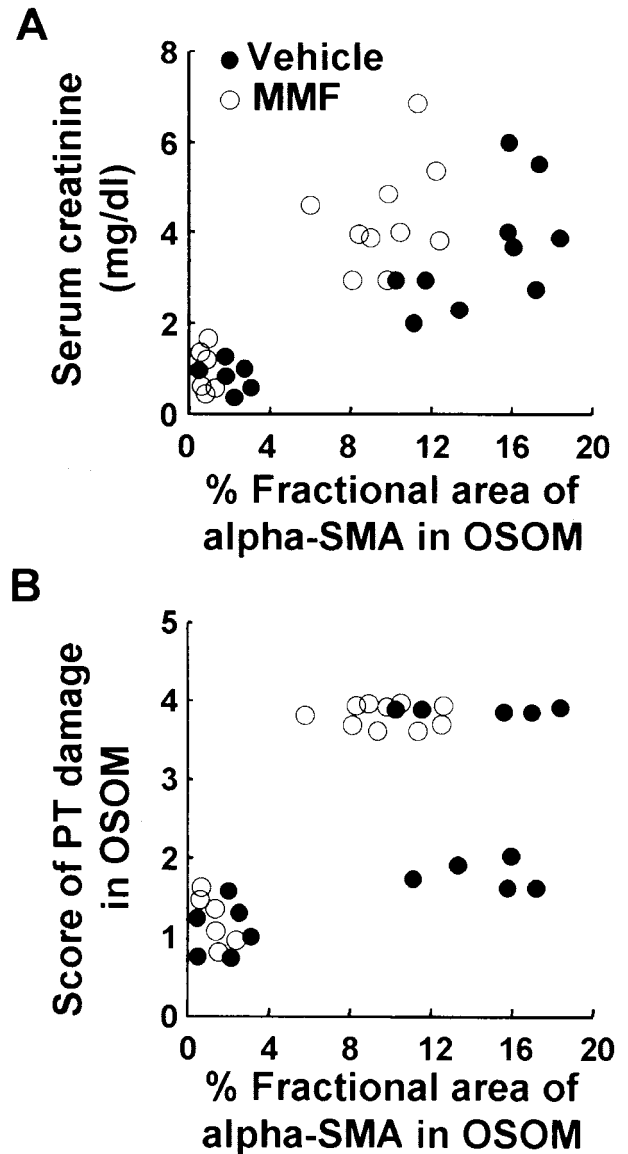


**Figure 9.** Correlation of percent fractional area of  $\alpha$ -SMA in OSOM to Scr and score of PT damage in vehicle and MMF groups. **A:** Percent fractional area of  $\alpha$ -SMA versus Scr;  $r = 0.81$  in vehicle group,  $P < 0.01$ ;  $r = 0.80$  in MMF group,  $P < 0.01$ . **B:** Percent fractional area of  $\alpha$ -SMA versus score of PT damage;  $r = 0.73$  in vehicle group,  $P < 0.01$ ;  $r = 0.65$  in MMF group,  $P < 0.05$ .

MMF treatment reduced the infiltration of macrophages and myofibroblasts at days 5 and 7, as judged by immunohistochemistry of ED1-positive macrophages and  $\alpha$ -SMA-positive myofibroblasts as well as expression of  $\alpha$ -SMA mRNA. MMF also reduced the number of cells positive for Ki67 (cell proliferation marker) in interstitial cells, although the cell type could not be identified because of technical limitations. As myofibroblasts initially appeared around the necrotic PT independent of macrophage infiltration, it is less likely that all reduction of myofibroblasts infiltration is secondary to the reduction of macrophages even though activated macrophages could contribute to fibroblast-myofibroblast phenotypic change and/or myofibroblast proliferation in certain pathological conditions.<sup>21,22</sup> Thus, it is possible that MMF



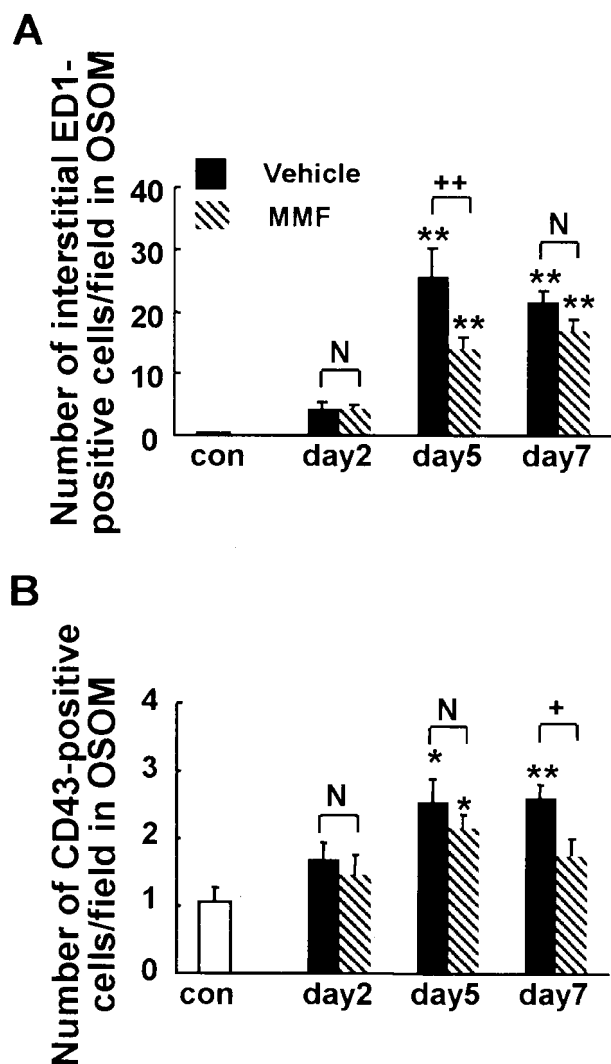


**Figure 10.** Morphometric analysis of the number of interstitial ED1-positive monocytes/macrophages (**A**) and CD43-positive lymphocytes (**B**) in OSOM in MMF-treated and vehicle-treated rats. Data represent the mean  $\pm$  SEM values of six rats. \*\*,  $P < 0.001$  versus normal control (con); N, no significant difference; +,  $P < 0.05$ ; ++,  $P < 0.001$ .

directly inhibited the infiltration of both macrophages and myofibroblasts.

In our study, MMF treatment inhibited the regenerative repair of PT as judged by BrdU- and Ki67-positive PT cells, and aggravated renal dysfunction as judged by Scr. However, we could not exclude a direct toxicity of MMF to regenerating PT cells. In this regard, MMF is well tolerated, with no reported nephrotoxicity, hepatotoxicity, myelosuppression, or other serious adverse effects.<sup>23</sup> Furthermore, MMF does not inhibit the regeneration of hepatocytes in rat hepatectomy model<sup>12</sup> and PT cells in rat ischemia/reperfusion model.<sup>11</sup> Based on these properties, it is likely that inhibition of PT regeneration noted in the present study is secondarily caused by inhibition of interstitial cellular response.

Our results also showed that MMF inhibited the infiltration of CD43-positive lymphocytes, a finding consistent with other studies.<sup>17,24</sup> However, the number of infiltrating lymphocytes was significantly reduced only at day 7 in

the MMF group compared with the vehicle group at the corresponding day, when regenerative repair had almost completed. Thus, it is less likely that lymphocyte infiltration mainly contributes to the initiation of PT regeneration.

It is reported that mononuclear leukocytes start to appear in the renal interstitium quite soon after the occurrence of ARF in both renal ischemic<sup>25</sup> and toxic<sup>7,26,27</sup> animal models. In the ischemia/reperfusion model, infiltrating leukocytes are considered to contribute to tissue damage.<sup>28</sup> To our knowledge, there is only one study that dealt with ARF and MMF treatment,<sup>11</sup> which reported that mycophenolic acid does not directly protect against ischemic injury in rats, but interferes with the injury response, through reduction in gene expression of RANTES (important in the chemotaxis of T-cells and macrophages) and allograft inflammatory factor (macrophage-associated cytokine), leading to reduction in renal injury. This conclusion emphasizes the contribution of infiltrating leukocytes to renal injury in the ischemia/reperfusion model. So far, only a few studies have examined the role of infiltrating leukocytes in the toxic model of ARF. Recently, Ghielli and colleagues<sup>29</sup> reported that inhibition of leukocyte infiltration induced by anti-adhesion molecule antibodies did not decrease tissue injury in HgCl<sub>2</sub>-induced ARF. Therefore, the role of leukocytes in the toxic model of ARF, particularly during the recovery phase remains unclear. Indeed, macrophages can produce several types of cytokines and growth factors, which promote epithelial cell proliferation, ECM turnover, and angiogenesis,<sup>30</sup> and act as important scavengers of apoptotic cells or necrotic cellular debris.<sup>31</sup> These are all necessary components of wound healing. Based on these known functions of macrophages, the present findings indicate that infiltrating macrophages may contribute to PT regeneration directly and/or indirectly in the UA-induced ARF model.

The rapid migration and proliferation of PT cells over a denuded TBM is an important PT repair response to injury. It is likely that myofibroblasts play an important role in this process, both because their location under TBM is ideal for paracrine action and because they can secrete the possible substances to enhance PT cell migration and proliferation. Myofibroblasts contain smooth muscle myosin isoforms in addition to  $\alpha$ -SMA actin, the requisite machinery for contraction and/or motility.<sup>5</sup> Thus, network formation of myofibroblast surrounding denuded TBM might protect the basement membrane by providing contractility and resisting the stretching force.<sup>32</sup> Myofibroblasts probably furnish ECM components to condition an environment for PT proliferation because they are known to play an essential role in synthesis and regulation of ECM components in wound healing.<sup>33</sup> These matrix proteins are the scaffold for tissue formation and growth, initiate intercellular signaling events through binding to cell receptor (integrins), and bind to growth factors and thus supply sustained concentration of these factors for epithelial cell migration, proliferation, and differentiation.<sup>34-36</sup> Moreover, myofibroblasts can provide growth factors in an autocrine and/or paracrine manner. Many of these factors may activate myofibroblasts themselves, resulting in myofibroblast motility and the release of ECM

proteins and other growth factors for inducing epithelial cell proliferation and differentiation.<sup>5</sup>

The beneficial roles for distinct growth factors such as epidermal growth factor, transforming growth factor (TGF)- $\alpha$ , fibroblast growth factor (FGF), hepatocyte growth factor, TGF- $\beta$ , and interleukin-1, possibly released by macrophages<sup>37,38</sup> and myofibroblasts<sup>35</sup> in renal repair of this model could be speculated. Epidermal growth factor and TGF- $\alpha$  belong to the same gene family, both act on the same epidermal growth factor receptor<sup>39,40</sup> and stimulate epidermal and dermal repair *in vivo*.<sup>41,42</sup> Exogenous epidermal growth factor administration *in vivo* enhances proliferation and accelerates recovery of damaged PTs after ischemia- or HCl<sub>2</sub>-induced kidney damage.<sup>43,44</sup> FGFs are mitogenic, angiogenic, and differentiation factors for epithelial and mesenchymal cells.<sup>5,45</sup> FGF-2 is potent mitogen for rat PT cells in primary culture.<sup>46</sup> Ichimura and colleagues<sup>47</sup> reported that FGF-1 and FGF-7<sup>48</sup> produced by renal interstitial cells may regulate epithelial cell growth during tubular repair in nephrotoxin-induced ARF model. Igawa and colleagues<sup>49</sup> reported that hepatocyte growth factor raised by renal interstitial cells and macrophages may function as a renotropic factor for renal regeneration after ischemia- or HgCl<sub>2</sub>-induced acute renal injury. Although TGF- $\beta$ 1 inhibits proliferation of rat PT cells *in vitro*,<sup>46</sup> the renal TGF- $\beta$ 1 mRNA level is reported to be up-regulated in regenerating PTs in the postischemic kidney.<sup>50</sup> As TGF- $\beta$  stimulates the expression of ECM proteins,<sup>51</sup> TGF- $\beta$ 1 may regulate ECM synthesis for renal tissue reconstruction in the postischemic kidney. In addition, TGF- $\beta$ 1 is a key factor mediating the transformation of fibroblasts to myofibroblasts<sup>28</sup> and is involved in the structural reorganization of the PT.<sup>52</sup> Interleukin-1 is identified as being involved in wound healing.<sup>53,54</sup> Interleukin-1 stimulates synthesis of renotropic cytokines such as hepatocyte growth factor and FGF-7<sup>55</sup> and may also act synergistically with TGF- $\beta$ 1 to induce the secretion of hepatocyte growth factor or FGF-7.<sup>56</sup>

In conclusion, we have demonstrated in the present study a transient appearance of interstitial cellular response including infiltration of both myofibroblasts and macrophages, after induction of ARF and that such response might play an important role in regenerative repair after UA-induced ARF.

## References

1. Weber KT: Fibrosis, a common pathway to organ failure: angiotensin II and tissue repair. *Semin Nephrol* 1997, 17:467-491
2. Badid C, Mounier N, Costa AM, Desmouliere A: Role of myofibroblasts during normal tissue repair and excessive scarring: interest of their assessment in nephropathies. *Histol Histopathol* 2000, 15:269-280
3. Muchaneta-Kubara EC, el Nahas AM: Myofibroblast phenotypes expression in experimental renal scarring. *Nephrol Dial Transplant* 1997, 12:904-915
4. Pierce GF, Mustoe TA, Lingelbach J, Masakowski VR, Griffin GL, Senior RM, Deuel TF: Platelet-derived growth factor and transforming growth factor-beta enhance tissue repair activities by unique mechanisms. *J Cell Biol* 1989, 109:429-440
5. Powell DW, Mifflin RC, Valentich JD, Crowe SE, Saada JI, West AB: Myofibroblasts. I. Paracrine cells important in health and disease. *Am J Physiol* 1999, 277:C1-C19
6. Leibovich SJ, Ross R: The role of the macrophage in wound repair. A study with hydrocortisone and antimacrophage serum. *Am J Pathol* 1975, 78:71-100
7. Sun DF, Fujigaki Y, Fujimoto T, Yonemura K, Hishida A: Possible involvement of myofibroblasts in cellular recovery of uranyl acetate-induced acute renal failure in rats. *Am J Pathol* 2000, 157:1321-1335
8. Eugui EM, Almquist SJ, Muller CD, Allison AC: Lymphocyte-selective cytostatic and immunosuppressive effects of mycophenolic acid *in vitro*: role of deoxyguanosine nucleotide depletion. *Scand J Immunol* 1991, 33:161-173
9. Gregory CR, Pratt RE, Huie P, Shorthouse R, Dzau VJ, Billingham ME: Effects of treatment with cyclosporine, FK 506, rapamycin, mycophenolic acid, or deoxyspergualin on vascular muscle proliferation *in vitro* and *in vivo*. *Trans Proceed* 1993, 25:770-771
10. Badid C, Vincent M, McGregor B, Melin M, Hadj-Aissa A, Veyseyre C, Hartmann DJ, Desmouliere A, Laville M: Mycophenolate mofetil reduces myofibroblast infiltration and collagen III deposition in rat remnant kidney. *Kidney Int* 2000, 58:51-61
11. Jones EA, Shoskes DA: The effect of mycophenolate mofetil and polyphenolic bioflavonoids on renal ischemia reperfusion injury and repair. *J Urol* 2000, 163:999-1004
12. Motale P, Mall A, Spearman CW, Lotz Z, Tyler M, Shepherd E, Kahn D: The effect of mycophenolate mofetil on liver regeneration. *Transplant Proc* 2001, 33:1054-1055
13. Yamaoka M, Hirata K, Ogata I, Tomiya T, Nagoshi S, Mochida S, Fujiwara K: Enhancement of albumin production by hepatocyte growth factor in rat hepatocytes: distinction in mode of action from stimulation of DNA synthesis. *Liver* 1998, 18:52-59
14. Houghton DC, Plamp III CE, DeFehr JM, Bennett WM, Porter G, Gilbert D: Gentamicin and tobramycin nephrotoxicity. A morphologic and functional comparison in the rat. *Am J Pathol* 1978, 93:137-152
15. Ghassemifar MR, Tarnuzzer RW, Chegini N, Tarpila E, Schultz GS, Franzen LE: Expression of alpha-smooth muscle actin, TGF-beta 1 and TGF-beta type II receptor during connective tissue contraction. *In Vitro Cell Dev Biol Anim* 1997, 33:622-627
16. Ishidoya S, Morrissey J, McCracken R, Reyes A, Klahr S: Angiotensin II receptor antagonist ameliorates renal tubulointerstitial fibrosis caused by unilateral ureteral obstruction. *Kidney Int* 1995, 47:1285-1294
17. Romero F, Rodriguez-Iturbe B, Parra G, Gonzalez L, Herrera-Acosta J, Tapia E: Mycophenolate mofetil prevents the progressive renal failure induced by 5/6 renal ablation in rats. *Kidney Int* 1999, 55:945-955
18. Fujihara CK, Malheiros DM, Zatz R, Noronha ID: Mycophenolate mofetil attenuates renal injury in the rat remnant kidney. *Kidney Int* 1998, 54:1510-1519
19. Shaw LM, Nowak I: Mycophenolic acid: measurement and relationship to pharmacologic effects. *Ther Drug Monit* 1995, 17:685-689
20. Johnson HJ, Swan SK, Heim-Duthoy KL, Nicholls AJ, Tsina I, Tar-nowski T: The pharmacokinetics of a single oral dose of mycophenolate mofetil in patients with varying degrees of renal function. *Clin Pharmacol Ther* 1998, 63:512-518
21. Diamond JR, van Goor H, Ding G, Engelmeyer E: Myofibroblasts in experimental hydronephrosis. *Am J Pathol* 1995, 146:121-129
22. Vyalov S, Desmouliere A, Gabbiani G: GM-CSF-induced granulation tissue formation: relationships between macrophage and myofibroblast accumulation. *Virchows Arch B Cell Pathol* 1993, 63:231-239
23. Schiff MH, Goldblum R, Rees MMC: 2-Morpholinoethyl mycophenolic acid in the treatment of refractory rheumatoid arthritis. *Arthritis Rheum* 1990, 33:S155
24. Remuzzi G, Zoja C, Gagliardini E, Corna D, Abbate M, Benigni A: Combining an antiproteinuric approach with mycophenolate mofetil fully suppresses progressive nephropathy of experimental animals. *J Am Soc Nephrol* 1999, 10:1542-1549
25. Takada M, Nadeau KC, Shaw GD, Marquette KA, Tilney NL: The cytokine-adhesion molecule cascade in ischemia/reperfusion injury of the rat kidney. Inhibition by a soluble P-selectin ligand. *J Clin Invest* 1997, 99:2682-2690
26. Ghielli M, Verstrepen WA, Dauwe S, Nouwen EJ, De Broe ME: Selective depletion of CD8-positive leukocytes does not alter mercuric chloride induced acute renal failure in the rat. *Exp Nephrol* 1997, 5:69-81

27. Xie Y, Nishi S, Iguchi S, Imai N, Sakatsume M, Saito A, Ikegame M, Iino N, Shimada H, Ueno M, Kawashima H, Arakawa M, Gejyo F: Expression of osteopontin in gentamicin-induced acute tubular necrosis and its recovery process. *Kidney Int* 2001, 59:959–974
28. De Greef KE, Ysebaert DK, Ghielli M, Vercauteren S, Nouwen EJ, Eyskens EJ, De Broe ME: Neutrophils and acute ischemia-reperfusion injury. *J Nephrol* 1998, 11:110–122
29. Ghielli M, Verstrepen WA, De Greef KE, Helbert MH, Ysebaert DK, Nouwen EJ, De Broe ME: Antibodies to both ICAM-1 and LFA-1 do not protect the kidney against toxic (HgCl<sub>2</sub>) injury. *Kidney Int* 2000, 58:1121–1134
30. Danon D, Kowatch MA, Roth GS: Promotion of wound repair in old mice by local injection of macrophages. *Proc Natl Acad Sci USA* 1989, 86:2018–2020
31. Aderem A, Underhill DM: Mechanisms of phagocytosis in macrophages. *Annu Rev Immunol* 1999, 17:593–623
32. Hinz B, Celetta G, Tomasek JJ, Gabbiani G, Chaponnier C: Alpha-smooth muscle actin expression upregulates fibroblast contractile activity. *Mol Biol Cell* 2001, 12:2730–2741
33. Sappino AP, Schurch W, Gabbiani G: Differentiation repertoire of fibroblastic cells: expression of cytoskeletal proteins as marker of phenotypic modulations. *Lab Invest* 1990, 63:144–161
34. Birchmeier C, Birchmeier W: Molecular aspects of mesenchymal-epithelial interactions. *Annu Rev Cell Biol* 1993, 9:511–540
35. Simon-Assmann P, Kedinger M, De Arcangelis A, Rousseau V, Simo P: Extracellular matrix components in intestinal development. *Experientia* 1995, 51:883–900
36. Schuppan D, Schmid M, Somasundaram R, Ackermann R, Ruehl M, Nakamura T, Riecken EO: Collagens in the liver extracellular matrix bind hepatocyte growth factor. *Gastroenterology* 1998, 114:139–152
37. Sunderkotter C, Steinbrink K, Goebeler M, Bhardwaj R, Sorg C: Macrophages and angiogenesis. *J Leukoc Biol* 1994, 55:410–422
38. Rappolee DA, Werb Z: Macrophage-derived growth factors. *Curr Top Microbiol Immunol* 1992, 181:87–140
39. Carpenter G, Cohen S: Epidermal growth factor. *J Biol Chem* 1990, 265:7709–7712
40. Fisher DA, Lakshmanan J: Metabolism and effects of epidermal growth factor and related growth factors in mammals. *Endocr Rev* 1990, 11:418–442
41. Schultz GS, White M, Mitchell R, Brown G, Lynch J, Twardzik DR, Todaro GJ: Epithelial wound healing enhanced by transforming growth factor-alpha and vaccinia growth factor. *Science* 1987, 235:350–352
42. Mustoe TA, Pierce GF, Morishima C, Deuel TF: Growth factor-induced acceleration of tissue repair through direct and inductive activities in a rabbit dermal ulcer model. *J Clin Invest* 1991, 87:694–703
43. Norman J, Tsau YK, Bacay A, Fine LG: Epidermal growth factor accelerates functional recovery from ischaemic acute tubular necrosis in the rat: role of the epidermal growth factor receptor. *Clin Sci* 1990, 78:445–450
44. Coimbra TM, Cieslinski DA, Humes HD: Epidermal growth factor accelerates renal repair in mercuric chloride nephrotoxicity. *Am J Physiol* 1990, 259:F438–F443
45. Hammerman MR, Rogers SA, Ryan G: Growth factors and metanephrogenesis. *Am J Physiol* 1992, 262:F523–F532
46. Zhang GH, Ichimura T, Wallin A, Kan M, Stevens JL: Regulation of rat proximal tubule epithelial cell growth by fibroblast growth factors, insulin-like growth factor-1 and transforming growth factor-beta, and analysis of fibroblast growth factors in rat kidney. *J Cell Physiol* 1991, 148:295–305
47. Ichimura T, Maier JA, Maciag T, Zhang G, Stevens JL: FGF-1 in normal and regenerating kidney: expression in mononuclear, interstitial, and regenerating epithelial cells. *Am J Physiol* 1995, 269:F653–F662
48. Ichimura T, Finch PW, Zhang G, Kan M, Stevens JL: Induction of FGF-7 after kidney damage: a possible paracrine mechanism for tubule repair. *Am J Physiol* 1996, 271:F967–F976
49. Igawa T, Matsumoto K, Kanda S, Saito Y, Nakamura T: Hepatocyte growth factor may function as a renotropic factor for regeneration in rats with acute renal injury. *Am J Physiol* 1993, 265:F61–F69
50. Basile DP, Rovak JM, Martin DR, Hammerman MR: Increased transforming growth factor-beta 1 expression in regenerating rat renal tubules following ischemic injury. *Am J Physiol* 1996, 270:F500–F509
51. Border WA, Ruoslahti E: Transforming growth factor-beta in disease: the dark side of tissue repair. *J Clin Invest* 1992, 90:1–7
52. Massague J: The transforming growth factor-beta family. *Annu Rev Cell Biol* 1990, 6:597–641
53. Sauder DN, Kilian PL, McLane JA, Quick TW, Jakubovic H, Davis SC, Eaglstein WH, Mertz PM: Interleukin-1 enhances epidermal wound healing. *Lymphokine Res* 1990, 9:465–473
54. Graves DT, Nooh N, Gillen T, Davey M, Patel S, Cottrell D, Amar S: IL-1 plays a critical role in oral, but not dermal, wound healing. *J Immunol* 2001, 167:5316–5320
55. Dinarello CA: Biologic basis for interleukin-1 in disease. *Blood* 1996, 87:2095–2147
56. Chedid M, Rubin JS, Csaky KG, Aaronson SA: Regulation of keratinocyte growth factor gene expression by interleukin 1. *J Biol Chem* 1994, 269:10753–10757